GEMINI

INTERFEROMETER

THEORETICAL MANUAL





NIREOS SRL

Via Giovanni Durando, 39 - 20158 Milan (Italy) info@nireos.com | www.nireos.com

This manual is continuously updated by our staff to help our customers to use the GEMINI interferometer at the top of its potential. You can always find the latest version of this manual at www.nireos.com/downloads

We made our best to assure that the manual is clearly written and does not contain errors, but we are aware of possible imperfections. Please contact us at info@nireos.com in case you spot an error or in case you find hard to understand some parts of the manual.

Subject to change without notice Document Version: 1.1-A

1 | Page

Contents

1.	Introduction								3
2.	GEMINI Interferometer working principle								
3.	Differences	with	respect	to	Michelson	interferometer:	wavelength	and	intensity
calil	bration								4

1. Introduction

The aim of this manual is to explain all the theoretical principle needed to properly understand the GEMINI interferometer working principle. The advantages of this technology are explained in comparison with other existing technology such as Michelson's interferometers.

2. GEMINI Interferometer working principle

The GEMINI interferometer consists of two polarizers (Pol1 and Pol2 in Fig. 1) and two birefringent optical elements (blocks A and B), with optical axes oriented perpendicular to the propagation direction of the beam (see yellow arrow and dots in Fig. 1). Pol1 is oriented at 45° with respect to these optical axes, meaning that the transmitted light can be described as the superposition of two replicas with perpendicular polarization and zero relative delay.

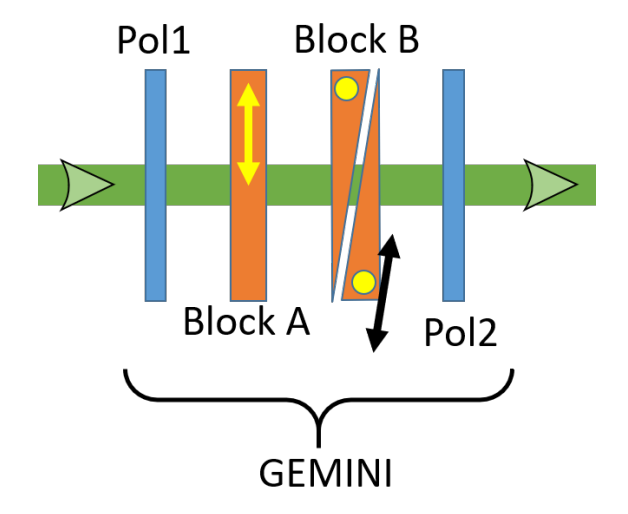


Figure 1 Simplified scheme of the GEMINI interferometer.

Block A introduces a delay au_{MAX} between these two fields equal to $au_{MAX} = \Delta n \cdot L / c$, where L is its thickness, $\Delta n = n_e - n_o$ is the birefringence of the crystal (i.e. the difference between the extraordinary and ordinary refractive indexes) and c is the speed of light in vacuum.

The optical axis of Block B is oriented orthogonally to block A, so that it reverts the delay and allows crossing the zero optical path difference. Block B is shaped in form of two wedges (with an apex angle α), thus acting as a plate with parallel faces and variable thickness.

One of the two wedges is mounted on a precision linear positioner, oriented along an axis x that creates an angle $\pi/2-\alpha$ with respect to the propagating light beam, so as to maintain constant the distance between the two wedges (as shown in Fig. 1). It is possible in this way to

control the relative delay of the two replicas with attosecond accuracy, according to the formula $\tau = \Delta n \cdot x \cdot \sin \alpha / c$.

Pol2, oriented as Pol1 at 45° with respect to the optical axes of the birefringent materials, finally projects the two replicas onto the same polarization state to ensure their interference at the detector.

3. Differences with respect to Michelson interferometer: wavelength and intensity calibration.

Considering the usual Fourier Transform (FT) spectroscopy using a Michelson's interferometer, the delay τ between the two replicas does not depend on the wavelength; therefore, one can readily obtain the spectrum $\tilde{S}(\nu)$ as a function of the optical frequency ν as:

$$\tilde{S}(v) = \int I(\tau)e^{i2\pi v\tau}d\tau$$

Where $I(\tau)$ is the interferogram that is given by:

$$I(\tau) = \int \left| \tilde{E}(v) + \tilde{E}(v) e^{-i2\pi\tau v} \right|^2 dv$$

Differently, using a birefringent interferometer, the delay τ is wavelength dependent due to the difference between the ordinary and extraordinary indexes of refraction, and it is given by: $\tau(\nu,x) = \frac{\Delta n(\nu) \cdot \sin \alpha \cdot x}{c}$ where $\Delta n(\nu)$ is the optical frequency-dependent birefringence, x is the wedge insertion, x is the speed of light in the vacuum and x is the wedge apex angle. Therefore, the recorded interferogram as a function of x is given by:

$$I(x) = \int \left| \tilde{E}(v) + \tilde{E}(v) e^{-i2\pi\tau(v,x)v} \right|^2 dv = \int \left| \tilde{E}(v) + \tilde{E}(v) e^{-i2\pi\frac{\Delta n(v)\sin\alpha \cdot x}{c}v} \right|^2 dv$$

From which the spectrum as a function of the spatial frequency $f_{\scriptscriptstyle x}$ can be calculated as:

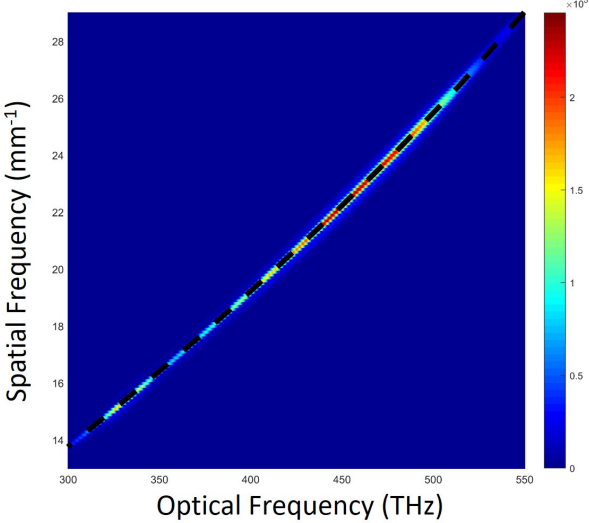
$$\tilde{S}(f_x) = \int I(x)e^{i2\pi f_x x} dx$$

Since the spatial frequencies depend on the parameters of the device such as the birefringence $\Delta n(v)$ and the apex angle α , it is very important to transform the retrieved entity $\tilde{S}(f_x)$ into

 $\tilde{S}(\nu)$. To do this we need first of all to find the function $\nu = F(f_x)$ that converts the abscissa values from spatial to optical frequency.

In order to find this relationship, we can consider a monochromatic wave with optical frequency \overline{v} entering the GEMINI interferometer. The recorded interferogram I(x) as a function of the wedge insertion x is a sinusoidal wave, with a spatial period $X = \frac{c}{\Delta n(\overline{v}) \times \sin \alpha \times \overline{v}} \text{. The FT of the interferogram } I(x) \text{ provides a spectrum } \widetilde{S}(f_x) \text{ as a function of spatial frequency } f_x, \text{ with a peak at } \overline{f_x} = \frac{\Delta n(\overline{v}) \times \sin \alpha \times \overline{v}}{c} \text{. If one repeats this procedure for a series of monochromatic waves, the result is a curve as a function of spatial frequency <math>f_x$ (vertical axis) and optical frequency v (horizontal axis) as the one shown in the figure below. In the same figure we have overlaid the computed calibration curve $\overline{f_x} = \frac{\Delta n(\overline{v}) \times \sin \alpha \times \overline{v}}{c}$ employing the well-known Sellmeier equations for the ordinary $n_0(v)$

and extraordinary $n_e(v)$ indexes of refraction of the birefringent material. The resulting curve (dashed black line) overlaps with the experimental one.



The calibration procedure aims at finding experimentally the function $v = F(f_x) = \frac{c \times f_x}{\Delta n(f_x) \times \sin \alpha}$ that maps the specific spatial frequency f_x to the corresponding

optical frequency ν . In this way, it is possible to easily convert the axis of the measured spectrum in the optical frequency domain and finally into the wavelength domain. This can be simply accomplished by using a polynomial fitting from a set of measurements obtained with known optical frequencies. This set of optical frequencies is obtained by using different

interferential filters or by using known laser lines or in a more accurate way by measuring the spectral interference at the output of the interferometer with a spectrometer as explained in [Perri *et al.*, "Excitation-emission Fourier-transform spectroscopy based on a birefringent interferometer," Opt. Express 25, A483-A490 (2017)].

After the polynomial interpolation we obtain a set of coefficients P_i such that $v = F(f_x) = \sum_{1}^{n} P_i f_x^i$. In this way, it is possible to convert the spatial frequencies axis into the corresponding optical frequencies axis, which is device independent. It is important to note that the calibration function is only dependent on the birefringent material and on the wedge apex angle. The calibrated curve obtained after this procedure is shown in the figure above.

Finally, we need to consider that an intensity calibration is also required to ensure energy conservation. To this purpose, we need to impose that $\tilde{S}(f_x)df_x=\tilde{S}(\nu)d\nu$, thus obtaining:

$$\tilde{S}(v) = \tilde{S}(f_x) \frac{df_x}{dv}$$

If we consider that $f_x=\frac{\Delta n(v)\sin\alpha v}{c}$ and $df_x=\frac{d\Delta n(v)}{dv}\frac{v\sin\alpha}{c}dv+\frac{\Delta n(v)\sin\alpha}{c}dv$, we arrive at the following relationship:

$$\tilde{S}(v) = \tilde{S}(f_x) \left(\frac{d\Delta n(v)}{dv} \frac{v \sin \alpha}{c} + \frac{\Delta n(v) \sin \alpha}{c} \right)$$

It is important to note that this intensity calibration does not play a role when the physical entities to be measured are expressed as ratios (trasmittance, absorbance, etc), since the numerator and denominator corrections cancel each other.

It is important to note that, the level of accuracy and interferometric stability reached by the GEMINI interferometer is very high compared to standard Michelson interferometer, due to the uncorrelated mechanical vibrations of the two mirrors and the difficulty in maintaining the required alignment of the moving mirror within a range of few μ rad. Indeed, in the GEMINI interferometer the two replicas travel along the same path and experiece the same perturbations from the environment. Therefore, the absolute arrival path of the two changes but not the relative path of difference, which is the important factor in Fourier transform

spectroscopy. The relative delay accuracy of the GEMINI interferometer has been demonstrated to be in the order of a few attoseconds.

The reproducibility of the interferometer is extremely high, this is due to the so called gear ratio factor which decreases the effective path length change in response of a movement of the moving wedge along the x axis. Indeed, in a Michelson's interferometer moving the moving mirror by an x amount increases the path length difference by two times this quantity (2x). In the GEMINI interferometer, moving the wedge by an x amount, introduces a pathlength difference of $\Delta n \cdot \sin \alpha \cdot x$. The factor $1/\Delta n \cdot \sin \alpha$ is the gear ratio of the interferometer which value is in the order of 50-60. Therefore, a positioning error introduces an error in the interferometric delay which is two orders of magintude less than the one of a Michelson's interferometer.

